

# Seismic modeling and analysis for sodium-cooled fast reactor

Gyeong-Hoi Koo\*, Suk-Hoon Kim and Jong-Bum Kim

*Korea Atomic Energy Research Institute, 1045 Daedeok-daero, Daejeon 305-353, Korea*

*(Received December 21, 2010, Revised June 1, 2012, Accepted August 7, 2012)*

**Abstract.** In this paper, the seismic analysis modeling technologies for sodium-cooled fast reactor (SFR) are presented with detailed descriptions for each structure, system and component (SSC) model. The complicated reactor system of pool type SFR, which is composed of the reactor vessel, internal structures, intermediate heat exchangers, primary pumps, core assemblies, and core support structures, is mathematically described with simple stick models which can represent fundamental frequencies of SSC. To do this, detailed finite element analyses were carried out to identify fundamental beam frequencies with consideration of fluid added mass effects caused by primary sodium coolant contained in the reactor vessel. The calculation of fluid added masses is performed by detailed finite element analyses using FAMD computer program and the results are discussed in terms of the ways to be considered in a seismic modeling. Based on the results of seismic time history analyses for both seismic isolation and non-isolation design, the functional requirements for relative deflections are discussed, and the design floor response spectra are proposed that can be used for subsystem seismic design.

**Keywords:** sodium-cooled fast reactor; seismic analysis; fluid added mass; seismic isolation

---

## 1. Introduction

The sodium-cooled fast reactor (SFR) investigated in this paper is the Advanced Burner Test Reactor (ABTR) (Chang 2006). The ABTR was developed at Argonne National Laboratory (ANL) as a first step in demonstrating technologies for the transmutation of transuranics recovered from Light Water Reactor (LWR) spent fuel, and hence, the benefits of fuel cycle closure to nuclear waste management. Additional ABTR objectives are to: 1) incorporate and demonstrate innovative design concepts and features that may lead to significant improvements in cost, safety, efficiency, reliability, or other favorable characteristics that could promote public acceptance and future private sector investment in Advanced Recycling Reactors (ARRs); 2) to demonstrate improved technologies for safeguards and security; and 3) to support development of the U.S. infrastructure for design, fabrication, and construction, testing, and deployment of systems, structures, and components for the ARRs.

The ABTR is a 95 MWe (250 MWt) metallic-fueled pool-type sodium-cooled fast reactor operating with core outlet and inlet temperatures of 510°C and 355°C, respectively. Most high

---

\*Corresponding author, Principal Researcher, Ph.D., E-mail: [ghkoo@kaeri.re.kr](mailto:ghkoo@kaeri.re.kr)

temperature reactor vessels cooled by the liquid metal are basically designed with a relatively thin thickness less than 5 cm to prevent excessive thermal bending stress caused by the elevated temperature service over 500°C (Kim 2009, Koo 2009). In general, liquid metal reactors are operated under lower design pressure less than 5 bars, therefore the thin thickness design is available. However, this design feature inevitably makes an issue related to the seismic design. To overcome this weakness of a thin thickness structural design, most liquid metal fast reactors tend to adapt the seismic isolation design concept (Micheli 2004, Forni 1994). Conclusively, the seismic design is one of main issues in SFR design and the technologies to construct the seismic analysis model are proposed in this paper.

Since the ABTR reactor system is a typical pool type SFR, the primary coolant system including the intermediate heat exchangers, pumps, and reactor internals is integrated into the reactor vessel. Therefore, the arrangement of components and the shape of reactor internals are not axisymmetric and are horizontally coupled together. Furthermore, since the coupled structures and components are submerged into a primary sodium coolant, their dynamic characteristics can be significantly affected by fluid added mass effects for different horizontal directions (Yang 1980, Su 1983, Frano 2009, Sigrist 2006). In this paper, the fluid added masses are calculated by detailed finite element analysis using the FAMD computer program (Koo 2003). And the application of these to the seismic modeling for this complicated system is described and discussed in detail.

From the established seismic analysis model, the time history response analyses are performed for the seismic isolation and non-isolation design conditions to investigate the functional requirement for relative deflections and to propose the design floor response spectra for seismic design of subsystems.

## **2. Design features of ABTR**

The ABTR is a pool type SFR with a 95 MWe reactor power and 60-year plant lifetime. The normal operating primary coolant temperatures are 355°C and 510°C at the core inlet and outlet, respectively. As shown in Fig. 1, the ABTR has reactor and guard vessels constructed of 316 austenitic stainless steel. The internal reactor vessel contains the reactor core, entire primary coolant, two intermediate heat exchangers, four primary pumps, four Direct Reactor Auxiliary Cooling System (DRACS) heat exchangers, and the accompanying internals. It has an inside diameter of 5.57 m, a wall thickness of 0.05 m, and an overall height of 13.35 m. The guard vessel is designed to hold the primary coolant in the event of a leak in the primary coolant system and to ensure that the inlets to the intermediate heat exchangers remain covered with sodium. The inside diameter of the guard vessel is 6.07 m, and the vessel thickness is 0.025 m. Therefore, the gap distance between the reactor vessel and the guard vessel is 0.2 m. The outer surface of the guard vessel is thermally insulated to reduce the heat lost to the guard vessel cooling system, which is designed to prevent overheating of the concrete support structure during normal and abnormal conditions.

The temperature regions of the primary coolant are designed to be divided into cold pool and hot pool regions by a complex redan structure. Actually, the redan structure has a main function, not only to separate the hot pool and cold pool regions, but also to protect the reactor vessel against thermal transient events. The gaps between the redan and the reactor vessel are 0.09 m and 0.65 m in region of the IHXs and the primary sodium pumps, respectively.

During normal operation, the cold pool free surface (CPFS) level is 2.04 m lower than the hot

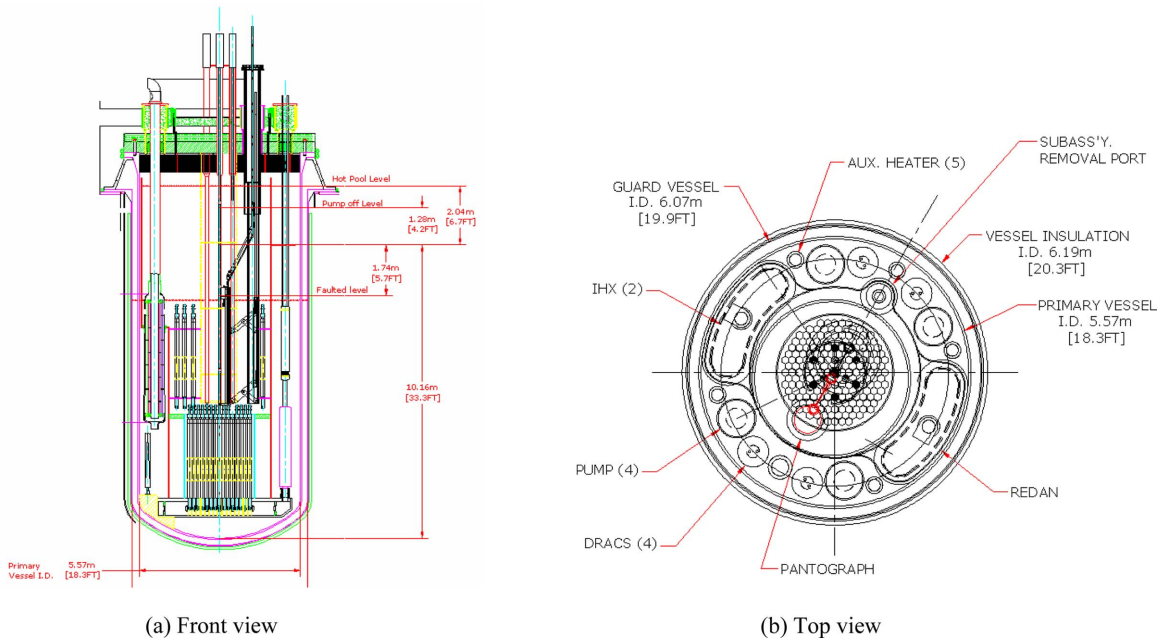


Fig. 1 Dimensions and layout of ABTR reactor

pool free surface (HPFS) level as indicated in Fig. 1(a). The space over the primary coolant free surface is filled with helium cover gas.

The seismic isolation is a seismic design strategy in which special structural elements are introduced to decouple a structural system from ground motion so that the damaging horizontal components of earthquake ground motions can not be transmitted into the system. In the ABTR design, the horizontal seismic isolation concept is adapted with the seismic isolator of the multiple friction pendulum system (MFPS). It consists of a lower and upper sliding surface, and two sliders in between the two sliding surfaces. While the total weight of the ABTR reactor structure is estimated to be 11000 metric tons, each isolator carries 600 tons. Therefore, a total of 20 isolators are used to support the reactor structure. The radius of curvature for the lower and upper sliding surfaces of the isolator is designed such that the period of the isolator is 3 seconds, and the maximum allowable seismic displacement is 30 cm.

### 3. Development of seismic analysis model

The seismic analysis model is developed by the simple stick model with beam element, concentrated mass element, and spring-damper element. This model has to describe the reactor building, which is isolated by the seismic isolators, and main structures and components including reactor vessel, reactor internals, upper internal structure, core support structure, core assemblies, intermediate heat exchangers (IHX), primary pumps and inlet pipes, reactor head, etc. This model will be used to calculate the seismic time history responses and generate the design floor responses for a detail seismic design of structures, system, and components.

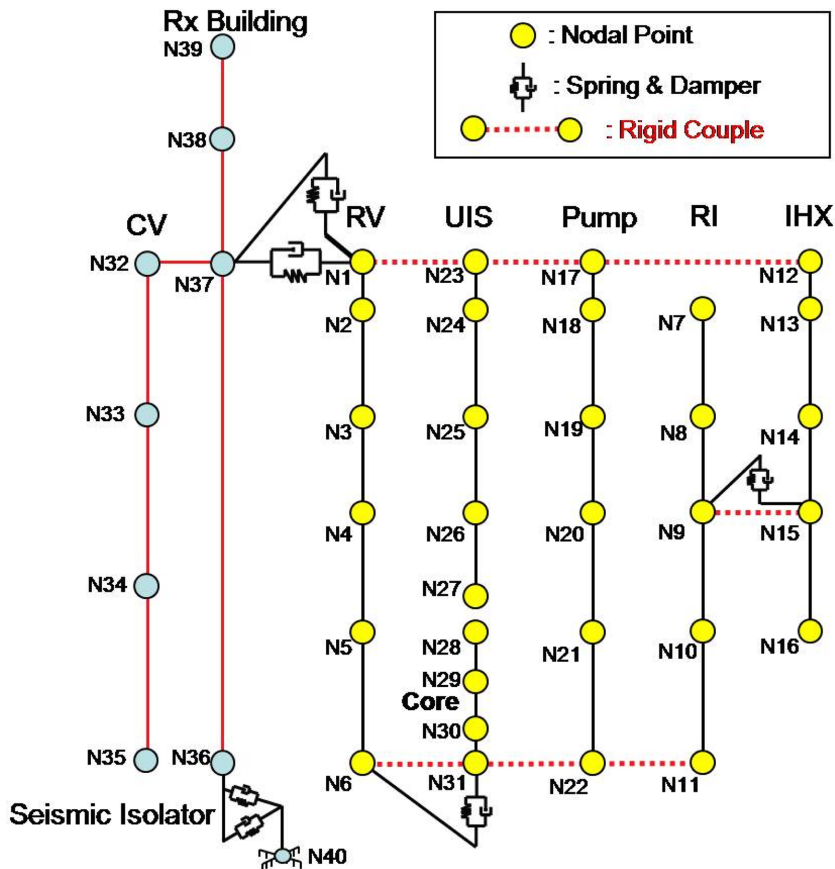


Fig. 2 Seismic analysis model for ABTR

The overall description of a seismic analysis model is shown in Fig. 2. The seismic analysis model totally consists of 40 numbers of node and 33 numbers of element. The reactor head, core support structure, and seismic isolators are modeled with spring-damper element. The dashed lines in the model indicate the coupled degree of freedom. The simple stick seismic analysis model is constructed by the detailed 3-dimensional finite element modal analyses for each component and structure to match the first beam modal frequency. The used main procedures to construct the whole seismic analysis model are as follows;

- Define the stick model for each component and structure
- Calculate the detailed fluid gap added mass for the submerged parts of components and structures by the FAMD code
- Establish the beam properties with equivalent mass density
- Perform the finite element modal analyses with detailed 3-dimensional model for each component and structure with consideration of fluid added mass effects
- Verify the fundamental beam frequency of each stick model with that of detailed finite element model
- Calculate the joint stiffness for reactor support, core support structure, and seismic isolation system

- Combine the each stick model with joint stiffness element and coupled nodal degree of freedom to construct the seismic analysis model
- Check and confirm the modal characteristics for the seismic analysis model

The detailed modeling methods and results are described for each component and structure in following sections. The used finite element program is a commercial ANSYS version 11.

### 3.1 Horizontal seismic analysis model

#### 3.1.1 Reactor vessel model

To identify the modal characteristics of the reactor vessel itself, the detailed 3-dimensional finite element model is established as shown in Fig. 3. The effects of the reactor core and internal structures will be included in a final seismic analysis model. In this model, the reactor vessel and the primary sodium coolant is modeled by the elastic shell element (SHELL63) and the 3-D acoustic fluid element (FLUID30) respectively. The total number of nodes and elements is 3921 and 3800, respectively. To consider the primary sodium coolant, it is assumed that the reactor vessel is filled with primary coolant up to the cold pool level contacting to reactor vessel. Then, the effects of fluid gaps between the components and internal structures are neglected. The fundamental beam modal frequency is revealed as 13.7 Hz for the reactor vessel.

The simple stick model for reactor vessel consists of six nodes as shown in Fig. 4. The beam properties such as a cross sectional area and area moment of inertia are  $0.88 \text{ m}^2$  and  $3.5 \text{ m}^4$ , respectively. The mass concentrated on node 1, which represents the reactor head including the rotating plug and insulation plate, is 30.42 tons. The element numbers 3 to 6 have a same

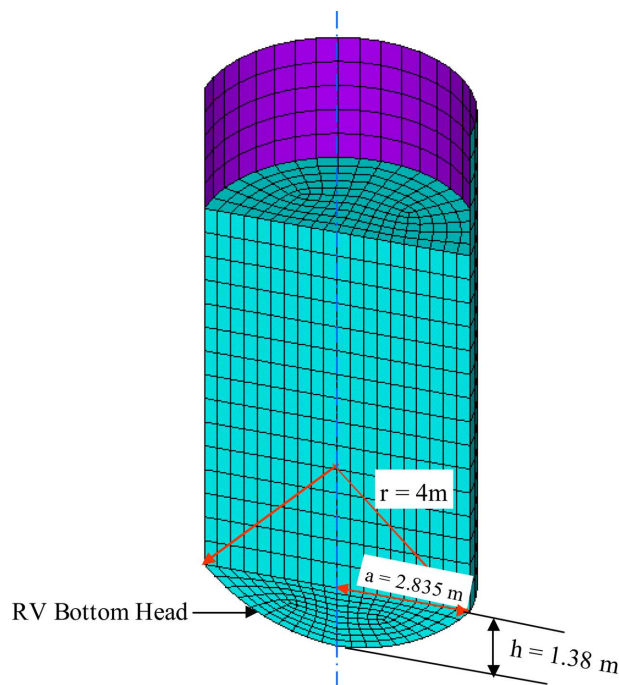


Fig. 3 Detailed finite element model for reactor vessel

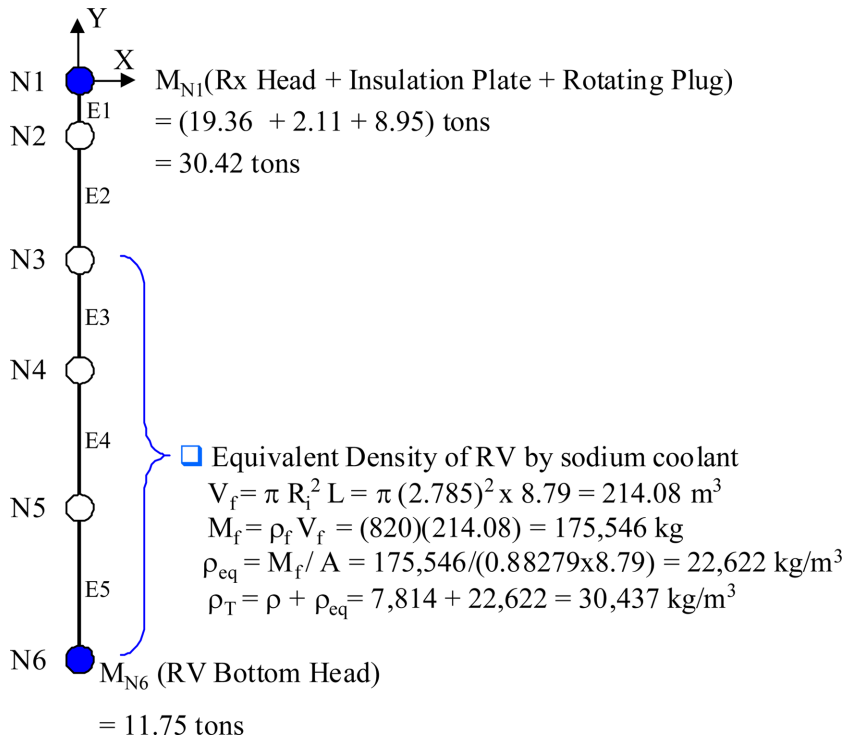


Fig. 4 Simple stick model of reactor vessel

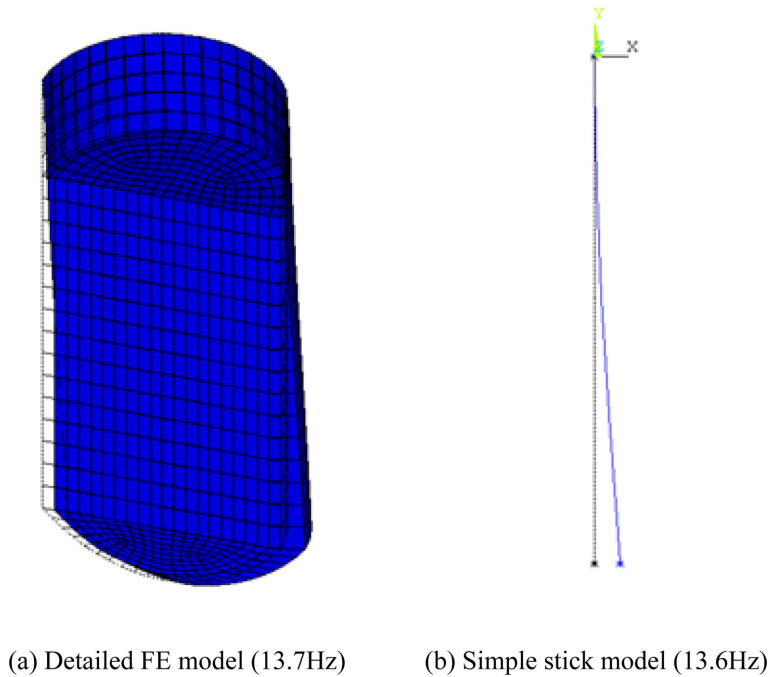


Fig. 5 Mode shapes of reactor vessel

equivalent mass density of  $30,473 \text{ kg/m}^3$  with consideration of primary sodium coolant and metal. The total mass and rotary mass moment of inertia for the bottom head of reactor vessel are 11.75 tons and  $3892 \times 10^3 \text{ kg}\cdot\text{m}^2$ , respectively and concentrated on node 6. Fig. 5 shows the comparison of fundamental mode shapes between the detailed model and the simple stick model. The calculated fundamental frequency 13.6 Hz is the same as that of the detailed finite element model.

### 3.1.2 Reactor internal model

Reactor internal of the ABTR is called as a redan wall structure fabricated with 316 stainless steel, which has a very complicated shape to accommodate the two kidney-type IHX components, fuel subassembly removal port located inside of redan wall and four primary pumps, four direct auxiliary cooling systems located outside of redan wall.

#### 3.1.2.1 Without fluid effects

The reactor internal in the air has shell mode shapes in fundamental frequencies. These shell modes do not affect the seismic responses for horizontal seismic input motions. Therefore, the stick model for time history analysis is constructed based on the beam modal characteristics. The beam modal frequencies for  $X$  and  $Y$  directions in air are 14.2 Hz for  $X$ -direction and 12.2 Hz for  $Y$ -direction due to the non-axisymmetric structural shape.

#### 3.1.2.2 With fluid effects

The fluid gaps around the reactor internal structure are very complicated due to the installed equipments and components and it is expected that the fluid added mass effects will be different from elevations along the redan wall. Therefore, it might be difficult to quantitatively define the fluid added masses along the elevation of a redan wall structure.

In this paper, the fluid added mass is considered by the equivalent mass density of structure with

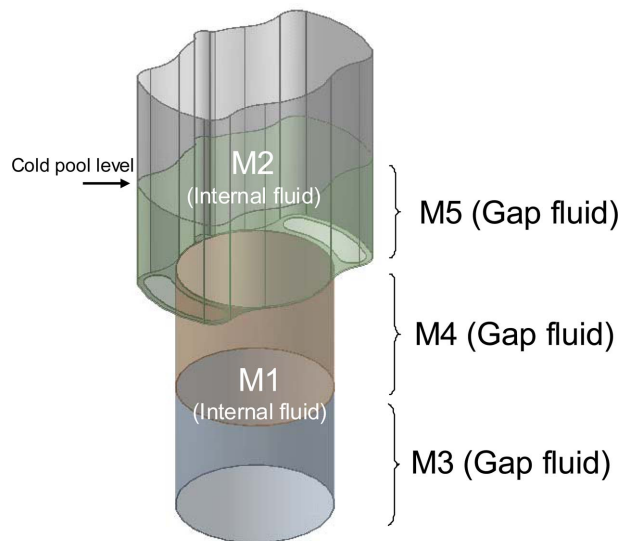


Fig. 6 Fluid regions for calculations of fluid added masses of RI

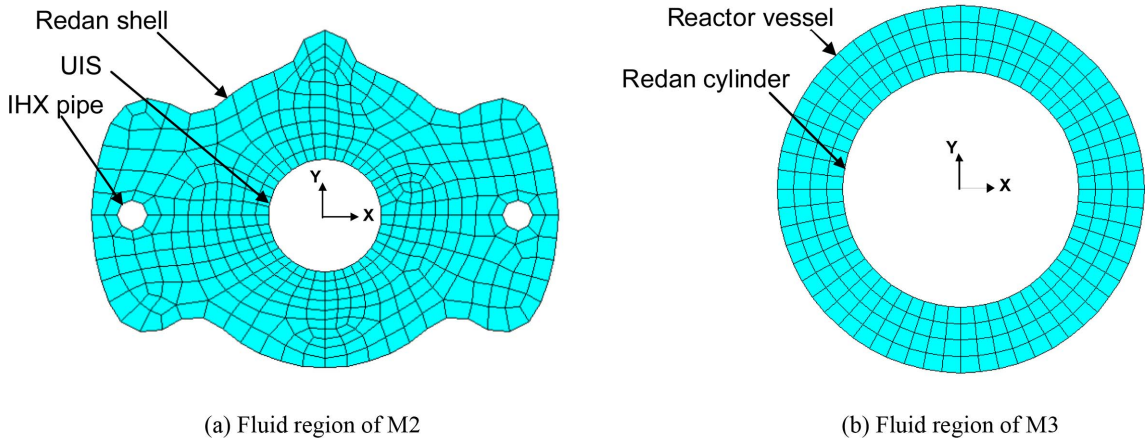


Fig. 7 Fluid regions for calculation of fluid added masses

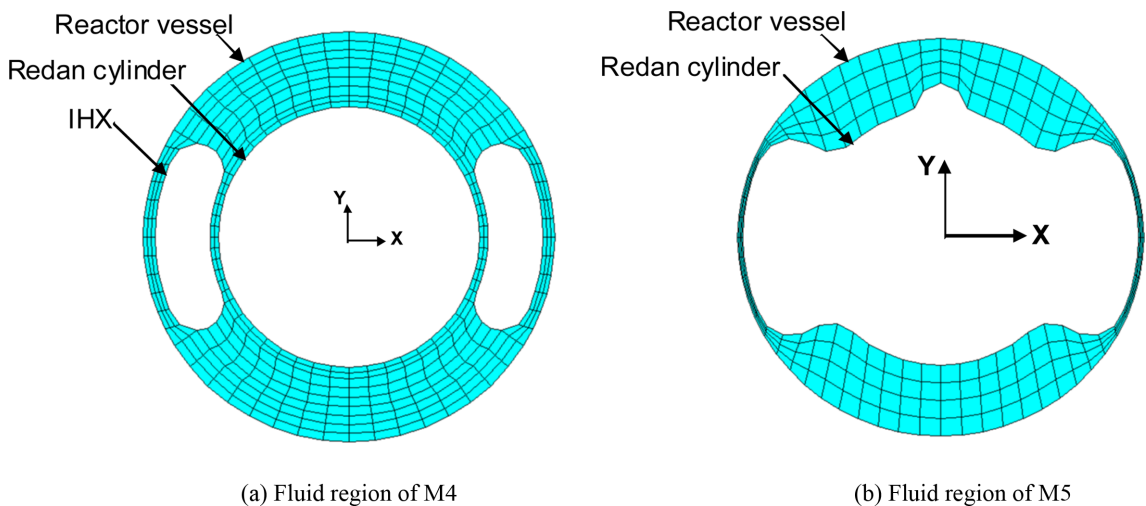


Fig. 8 Fluid regions for calculation of fluid added masses

five regions along the elevation as shown in Fig. 6. To quantify the equivalent densities, five regions are considered for the evaluations of fluid added mass effects applied to the redan wall structure. In the figure, the fluid added mass M1 and M2 are for internal fluid contained in lower cylinder and the upper shell respectively and M3 through M5 are the fluid added mass due to the fluid gaps between redan wall and around structures.

For the lower cylinder (M1), it is simply assumed that the inside cylinder is filled with 60% internal fluid with consideration of occupation of core assembly structures. The fluid added mass due to internal fluid contained in the upper shell (M2) is calculated by the detailed finite element analysis using the FAMD program. Fig. 7 and Fig. 8 show the 2-dimensional finite analysis models used to calculate the fluid added mass. In analysis model of Fig. 7(a), the upper internal structure (UIS) and two pipe lines of the IHXs are included. For a region of M3 of lower part cylinder, the

fluid added mass due to fluid gap between redan cylinder and the reactor vessel is calculated by using the finite element model as shown in Fig. 7(b). The obtained fluid added mass per unit area is  $M_f = 20,543 \text{ kg/m}$ . This can be compared with that by the theoretical formula for a co-axial cylinder. The theoretical formula is

$$\begin{Bmatrix} F_{x1} \\ F_{x2} \end{Bmatrix} = \begin{bmatrix} \alpha M_1 & -(1 + \alpha)M_1 \\ -(1 + \alpha)M_1 & (1 + \alpha)M_1 + M_2 \end{bmatrix} \begin{Bmatrix} a_{x1} \\ a_{x2} \end{Bmatrix}$$

where  $a = (R_2^2 + R_1^2)/(R_2^2 - R_1^2)$ ,  $M_1 = \rho\pi R_1^2$ , and  $M_2 = \rho\pi R_2^2$ . The calculated value by formula, 20,616 kg/m is good agreement with that by the detailed finite element analysis. For a region of M4 of lower part cylinder, the redan cylinder is surrounded by the reactor vessel and two IHXs as shown in a finite element model of Fig. 8(a). Due to the non-symmetric of fluid gaps around redan cylinder, the fluid added mass is different from  $X$ -direction to  $Y$ -direction. The fluid added masses per unit length are 30,026 kg/m for  $X$ -direction and 51,150 kg/m for  $Y$ -direction respectively. For a region of M5, the gap between redan wall and reactor vessel is partly filled with cold sodium. With assumption of fully submerged redan wall, the finite element model can be used as shown in Fig. 8(b). The calculated fluid added mass for M5 region is very large but, it is based on the assumption that the structure is fully submerged in coolant without consideration of the cold pool free surface. As expected from the non-symmetric geometry of redan shown in Fig. 7 and Fig. 8, we can see that  $Y$ -direction fluid added mass is much larger than that of  $X$ -direction. Even though the  $X$ -direction fluid gap between redan wall and reactor vessel is much smaller than the  $Y$ -direction, much larger fluid resistant surface in  $Y$ -direction invokes much more significant fluid added mass effect to that direction.

Actually, the method used in this calculation of a fluid added mass is 2-dimensional finite element analysis fundamentally based on the assumption that the structures are fully submerged and no flow effect to vertical direction. Therefore, there may be uncertainties in modeling of fluid added mass effects on redan wall structure, which has hot and cold coolant free surface contacting to upper gas region. To investigate the sensitivity of the fluid added mass effects on natural frequencies, case

Table 1 Summary of case studies for fluid added mass exerted on reactor internal

	$X$ -Direction, Hz	$Y$ -Direction, Hz	Equivalent Density
Case 1 (Air)	14.233	12.197	$\rho_{upper} = \rho_{lower} = 7787$
Case 2 (M1+M2)	5.086	4.345	$\rho_{upper} = 61,734$ $\rho_{lower} = 29,910$
Case 3 (M1+M2+M3)	4.994	4.305	$\rho_{upper} = 61,734$ $\rho_{lower} = 123,058$
Case 4 (M1+M2+M3+M4)	4.953	4.247	$\rho_{upper} = 61,734$ $\rho_{lower1x} = 123,058; \rho_{lower2x} = 166,064$ $\rho_{lower1Y} = 123,058; \rho_{lower2Y} = 261,851$
Case 5 (M1+M2+M3+M4+M5)	3.360	1.503	$\rho_{upper1x} = 316,162; \rho_{upper2x} = 61,734$ $\rho_{upper1Y} = 1,668,094; \rho_{upper2Y} = 61,734$ $\rho_{lower1x} = 123,058; \rho_{lower2x} = 166,064$ $\rho_{lower1Y} = 123,058; \rho_{lower2Y} = 261,851$

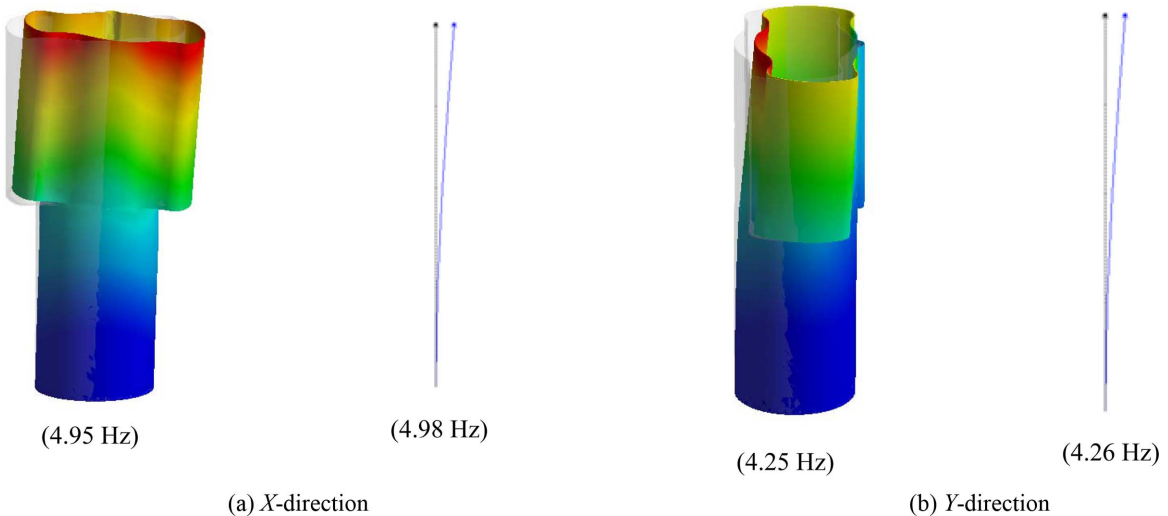


Fig. 9 Comparison of mode shapes for reactor redan wall

studies were performed for the calculated values for five fluid regions.

Table 1 presents the summary results of fundamental frequency analyses for five cases. Case 1 is for an air condition. The fundamental natural frequencies are 14.2 Hz for  $X$ -direction and 12.2 Hz for  $Y$ -direction respectively. Case 2 is just for considering the internal fluid effects contained inside redan wall. Case 3 is for considering the internal fluid and outer fluid of M3 region. The case 4 includes the fluid added masses by internal fluid of M1 and M2 regions and by fluid gaps in regions of M3 and M4. Case 5 considers all fluid added mass effects including M1 through M5 regions. As shown in the table, when the fluid added mass effects are considered, the fundamental natural frequencies drop down significantly from 12.2 Hz to 1.5 Hz for the case 5 in  $Y$ -direction. Therefore, we can see that the fluid added mass effects can significantly affect the dynamic behavior of reactor internal structure.

For the seismic analysis model, the fluid added mass effect at region M5 is excluded due to the uncertainties contained in the theoretical background of FAMD program, which is applicable for the fully submerged structures. Actually, it is necessary to verify the fluid added mass effects for partially submerged structures especially in sodium-cooled fast reactors, which inevitably have a coolant free surface in hot and cold primary coolant pool.

In this study, Case 4 in Table 1 is taken to be used for a simple stick model. Fig. 9 shows the comparison results of fundamental beam mode shapes for  $X$  and  $Y$  directions between detailed finite element model and simple stick model. The fundamental natural frequencies by stick model are 4.98 Hz for  $X$ -direction and 4.26 Hz for  $Y$ -direction, respectively. These are very good agreement with those by the detailed finite element models.

### 3.1.3 Intermediate heat exchanger model

In ABTR, there are two IHXs arranged along the  $X$ -direction as shown in Fig. 1(b). These two components are laterally coupled with reactor internals. To represent the beam mode shapes of a coupled IHXs by a single stick model, the coupled stick model is developed through the following procedures:

- Calculate fundamental beam natural frequencies by detailed finite element model for a single IHX
- Define a single component stick model
- Calculate total sectional area for two IHXs
- Calculate total area moment of inertia for coordinates of reactor center for two IHXs
- Define coupled IHX model

### 3.1.3.1 Single component model

The fundamental natural frequencies obtained from a detailed finite element model in air condition are 1.44 Hz for  $X$ -direction and 1.42 Hz for  $Y$ -direction respectively. For the fluid added mass along the IHX, two parts are considered. One is the IHX pipe and the other is IHX shell. The fluid added mass is calculated from the FAMD analysis using the model of Fig. 7(a) for IHX pipe and Fig. 8(a) for IHX shell respectively.

Table 2 presents the summary of IHX fundamental beam frequency analysis for air condition and fluid condition. In air condition, the fundamental frequencies of  $X$  and  $Y$  direction are almost same as 1.44 Hz and 1.42 Hz respectively. However, in fluid condition, the  $X$ -direction frequency is 0.318 Hz much lower than 0.761 Hz of  $Y$ -direction due to the difference of fluid added mass effects. This means that the fluid resistance toward  $X$ -direction is greater than  $Y$ -direction as presented in the calculation results of fluid added masses.

Fig. 10 presents the comparison of mode shape and fundamental frequency between a detailed finite element model and a simple stick model with consideration for fluid added mass effects. As shown in the results, the fundamental frequencies by a stick model are 0.316 Hz for  $X$ -direction and 0.764 Hz for  $Y$ -direction, respectively. These are very good agreement with those obtained by the detailed finite element model.

### 3.1.3.2 Coupled stick model

To consider the coupled beam properties for two IHXs arranged as shown in Fig. 1(b) of top view, the total sectional area and area moment of inertia for IHX piping and Shell are calculated as follows;

$$\begin{aligned} \text{Total Area: } A_t &= A \times 2 \\ \text{Total Area Moment of Inertia: } I_{yy} &= (1 + AR_x^2) \times 2 \\ I_{xx} &= I \times 2 \end{aligned}$$

where,  $A$  and  $I$  indicates an area and area moment of inertia for single IHX respectively, and  $R_x$  is the distance from rotational axis to center of IHX. This coupled stick model will be used for a seismic analysis model in Fig. 2.

Table 2 Summary of modal analyses for IHX

	$X$ -Direction, Hz	$Y$ -Direction, Hz
In Air	1.4402	1.4189
In Fluid	0.3176	0.7612

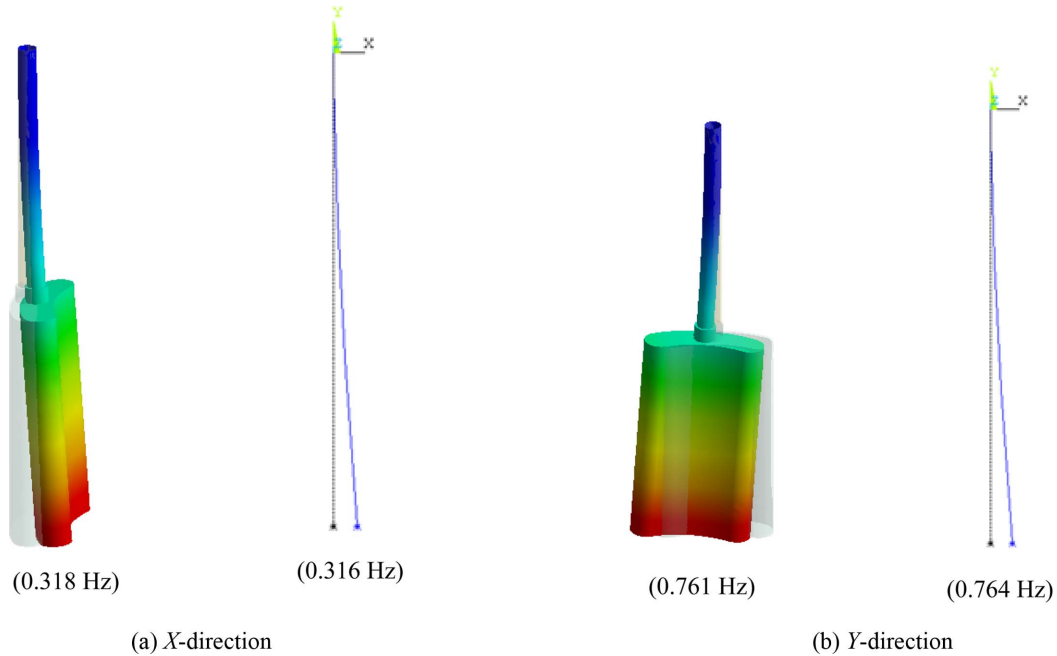


Fig. 10 Comparison of mode shapes of IHX in fluid

### 3.1.4 Primary pump and piping model

In ABTR design, there are four primary pumps jointed with the inlet piping in cold pool region. The procedures to develop the coupled stick model for four components are the same as above IHX model. Fig. 11 shows the 3-D CAD model of primary pump and internal piping. This model includes the pump, rotor shaft, outer cylinder, and inlet piping. The total height of the model is 14.2 m, and for the boundary conditions, all displacements of top end is constrained and the bottom end is horizontally constrained allowing vertical movement for thermal expansion.

The simple stick model is constructed with concentrated added mass of pump casing and blade at node number 20. Fig. 12 presents the comparison between mode shapes and fundamental frequencies obtained by detailed finite element model and simple stick model. As shown in the figures, the fundamental natural frequency obtained by a simple stick model is 4.9 Hz which is almost same as 4.94 Hz of 3-D finite element model.

For the coupled stick model representing four pump components, the total area and area moment of inertia are calculated as the same way for IHX and are used for the seismic analysis model of Fig. 2.

### 3.1.5 Upper internal structure model

The upper internal structure (UIS) is designed to accommodate various guideline tubes and provide a primary coolant mixing zone. In this study, only outer cylinder is considered without internal guide tubes and support structures. The UIS has a slot providing a space for in-vessel inspection machine (IVIM) to reach the core center region. The seismic stick model for UIS is described with five nodes as shown in Fig. 2. With consideration of a slot part in UIS, the equivalent elastic modulus,  $E_{eq} = 112$  GPa is used. The fundamental natural frequency obtained by a stick model is

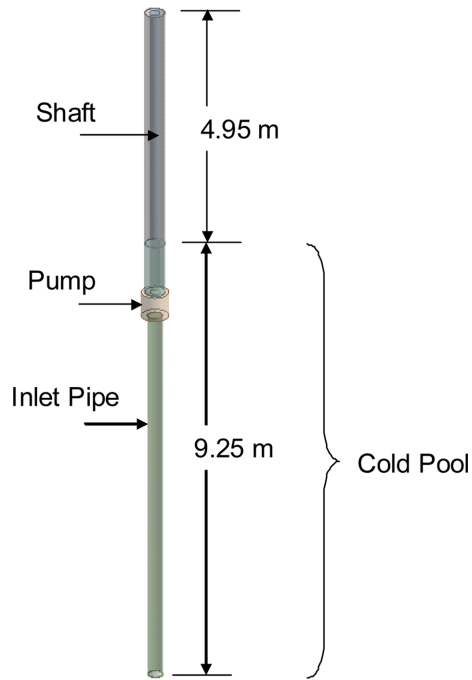


Fig. 11 Dimensions and shape of primary pump and internal piping

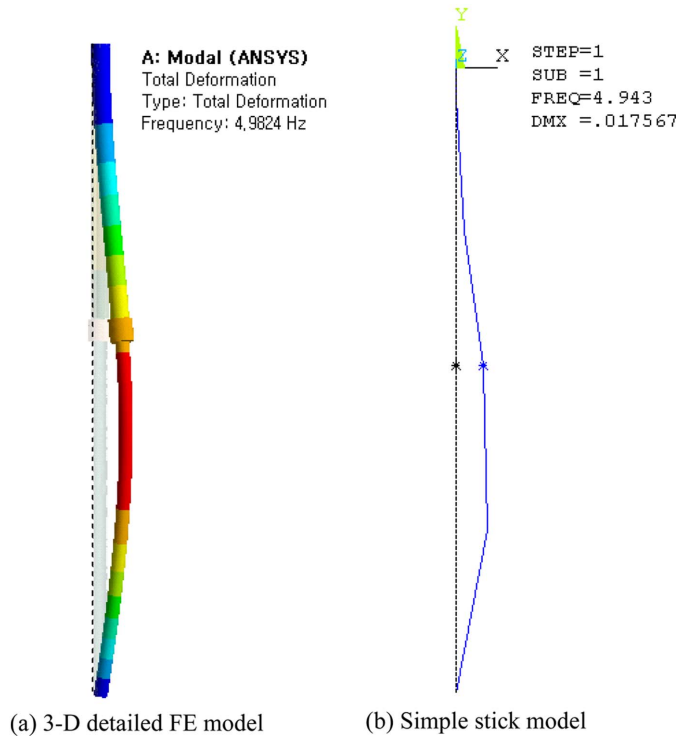


Fig. 12 Mode shapes of primary pump and inlet piping

13.16 Hz, and this is very good agreement with 13.11 Hz obtained by a detailed finite element model.

### 3.1.6 Core assembly model

For a seismic stick model of core assembly, a single core assembly is modeled to represent a core dynamic motion, and it is assumed that 200 tons of effective core assembly mass is concentrated on a core support structure (Node 31) to provide a total inertia mass of core assemblies to an assembled seismic analysis model.

The fuel assembly has an overall length of 328 cm and the duct thickness and the flat-to-flat length are 0.4 cm and 14.2 cm, respectively as shown in a top view of hexagonal shape of core duct with nose piece at the bottom end in Fig. 13.

The general assumptions used in modeling are as follows;

- All ducts have uniform sectional properties.
- The ducts/clusters have a cantilever support at the bottom end.
- Added mass effects of sodium along ducts are assumed as 10% increase of duct density.
- Core shroud attached to the core support plate has a rigid body motion, i.e. there is no relative motion between core shroud and core support plate.
- Sodium damping and squeeze film damping are ignored.
- No information concerning assembly bowing due to thermal and neutron flux gradients are available so all assemblies are assumed as a straight beam.

The beam properties for duct and nosepiece are as follows;

- for Duct

$$A_D = 2\sqrt{3}(DT - T^2) = 2\sqrt{3}(0.14198 \times 0.004 - 0.004^2) \\ = 1.9119 \times 10^{-3} \text{ m}^2$$

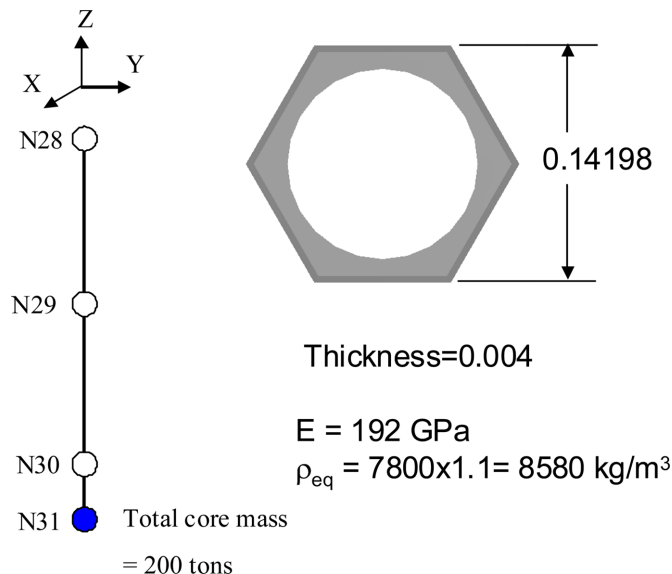


Fig. 13 Seismic stick model of core assemblies

$$I_D = \frac{5}{48\sqrt{3}}[D^4 - (D - 2T)^4] = \frac{5}{48\sqrt{3}}[0.14198^4 - (0.14198 - 2 \times 0.004)^4]$$

$$= 5.06 \times 10^{-6} \text{ m}^4$$

- for Nosepiece

$$A_N = \frac{\pi}{4}(D_o^2 - D_i^2) = \frac{\pi}{4}(0.122^2 - 0.114^2)$$

$$= 1.482 \times 10^{-3} \text{ m}^2$$

$$I_N = \frac{\pi}{64}(D_o^4 - D_i^4) = \frac{\pi}{64}(0.122^4 - 0.114^4)$$

$$= 2.5825 \times 10^{-6} \text{ m}^4$$

The obtained fundamental natural frequencies is 10.77 Hz for a simple stick model and 10.41 Hz the detailed finite element model. Both are in a good agreement.

### 3.1.7 Guard vessel model

The overall height of a guard vessel is 12.18 m and the outer diameter is 6.152 m. A simple seismic stick model for the guard vessel is constructed with four nodes as shown in Fig. 2. It is assumed that the total mass of the bottom head, 6.83 tons is concentrated on the node 35 (N35). The calculated fundamental natural frequency by a simple stick model is 26.9 Hz, and it is very good agreement with 26.7 Hz by a detailed finite element model.

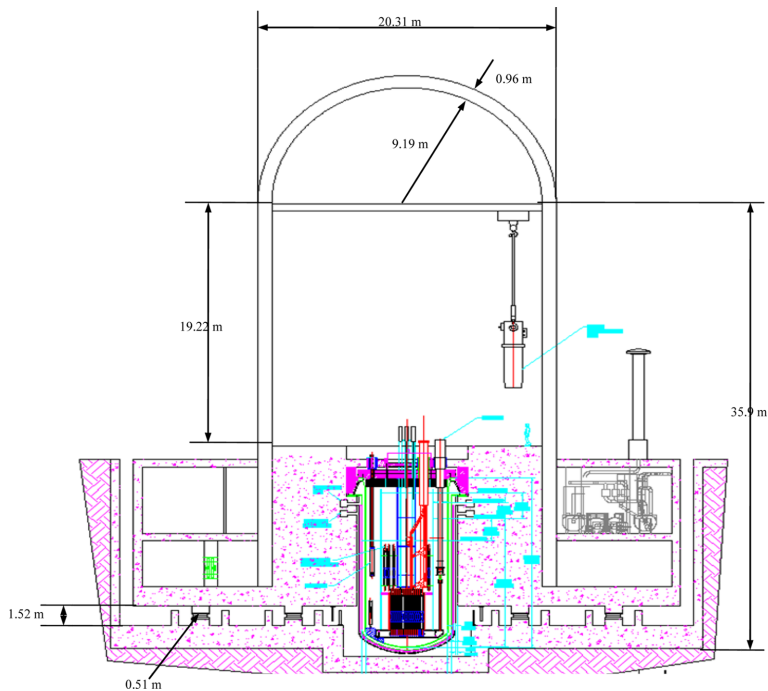


Fig. 14 Dimensions and layout of reactor building of ABTR

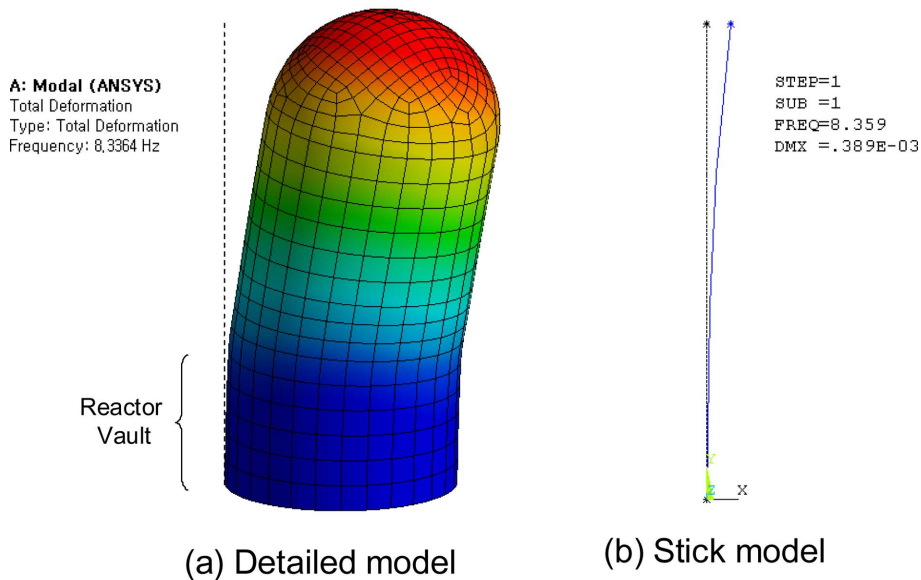


Fig. 15 Mode shapes of reactor building

### 3.1.8 Reactor building model

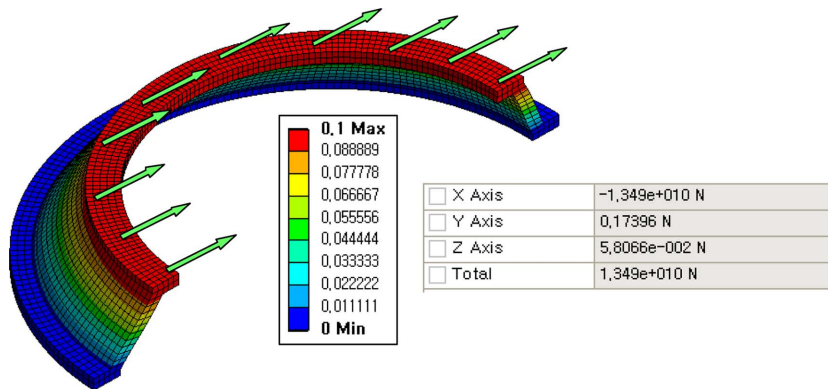
Actually, the finite element modeling of the reactor building with inclusion of various floor and structures is complicate (Lo Frano *et al.* 2010). Fig. 14 shows an overall layout and dimensions of ABTR reactor building. The total height from base plate to top of dome head is 46.04 m. The outer diameter and the wall thickness of the reactor building are 20.31 m and 0.96 m, respectively. As shown in figure, the reactor vault is very thick and fully filled with concrete. Then, the containment structure above the reactor vault is considered as a simple cylinder with hemispherical top head.

A simple seismic stick model for a reactor building is constructed with four nodes as shown in Fig. 2. It is assumed that the total mass of the dome head is concentrated on the node 39 (N39). The calculated fundamental natural frequency by a simple stick model is 8.4 Hz and in very good agreement with 8.3 Hz obtained by a detailed 3-D finite element analysis. Fig. 15 presents the mode shapes obtained by both analysis models. As shown in the figures, the part of a reactor vault reveals almost rigid body motion.

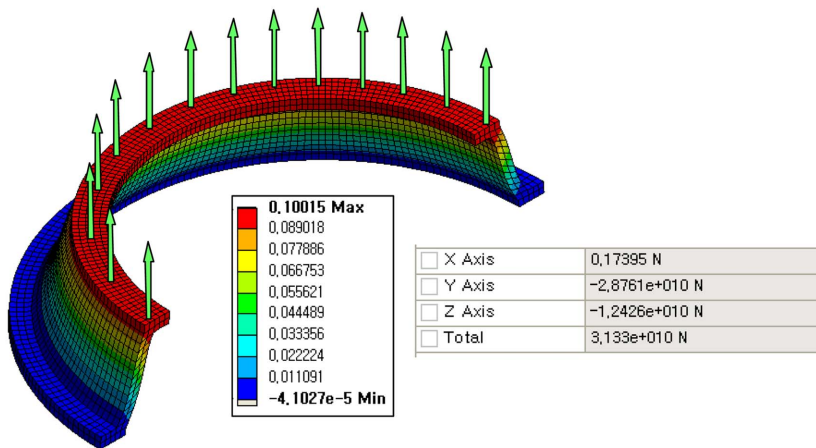
### 3.1.9 Reactor support structure model

The reactor support structure in ABTR is a skirt structure type. This is described by a simple stiffness element in the overall seismic stick model connecting the reactor building (Node 37) and the reactor head (Node 1). The half symmetric finite element models are used for a stiffness analysis. The method uses the unit displacement applying to the top flange, which is bolted with a reactor head and obtains the total reaction force at the bottom flange bolted with a concrete reactor vault.

Fig. 16 shows the stiffness analysis results for horizontal and vertical displacement loads, respectively. The calculated stiffness is 135 GN/m for horizontal and 313 GN/m for vertical, respectively. From the stiffness calculations, it is found that the designed reactor support has sufficient stiffness for horizontal and vertical directions.



(a) Horizontal direction



(b) Vertical direction

Fig. 16 Results of stiffness analysis for Rx support

### 3.1.10 Core support structure model

The core assemblies are vertically supported at the lower grid plate of the inlet plenum structure. Therefore, the seismic loads are expected to be dominantly transferred to core through a lower grid plate. The thickness of the lower grid plate is 5 cm and the horizontal stiffness is assumed to be rigid. To calculate the vertical stiffness of the lower grid plate the detail 3D finite element model is used with the assumption that the maximum deflection of the lower grid plate due to the core assemblies occurs at the center of the plate with the conservative deflection shape of the core assemblies and the lower grid plate as shown in Fig. 17. For the boundary conditions, the unit displacement is applied at a center point of the lower grid plate, and all displacements are

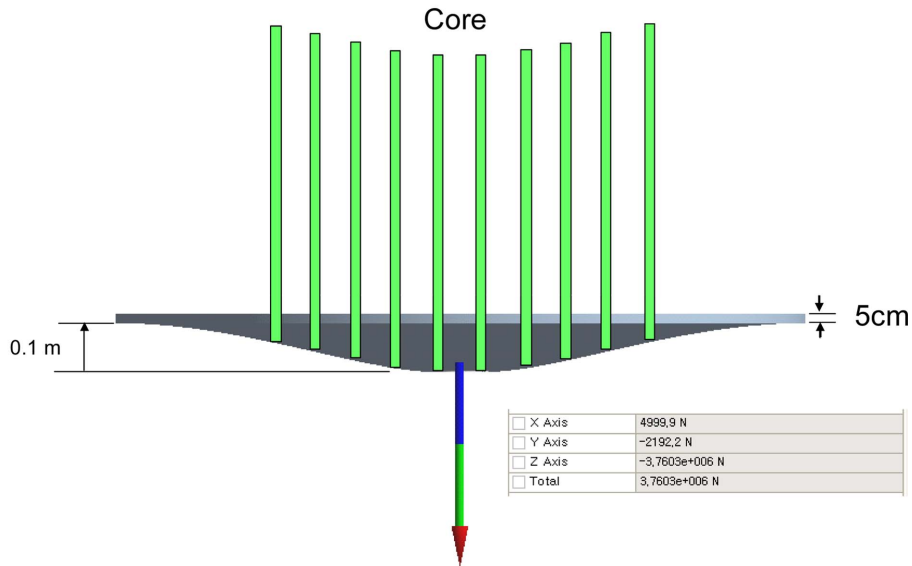


Fig. 17 Results of stiffness analysis for core support structure

constrained at the edge. The calculated vertical stiffness of the lower grid plate is 37.6 MN/m and reveals excessive vertical flexibility to support the core assemblies.

### 3.1.11 Seismic isolator model

Seismic isolators can be classified as either elastomeric or sliding. Elastomeric isolators include high-damping rubber bearing (HDRB) or lead inserted low-damping rubber bearing (LLRB). Sliding isolators include flat assemblies, the friction pendulum system (FPS) or the multiple friction-pendulum system (MFPS). For the ABTR's seismic isolation design, the sliding isolators are chosen in favor of the elastomeric isolators. Among the sliding isolators, MFPS is chosen to be used in the ABTR. The used mathematical model for a seismic isolator is a simple equivalent spring-damper model.

For the horizontal seismic isolation design of ABTR, the isolation frequency is required as 0.333 Hz (3 seconds), and the critical damping ratio of isolator for 0.3 g Peak Ground Acceleration (PGA) is assumed to be 5%. From this isolation frequency the horizontal stiffness,  $K_H$  and damping value,  $C_H$  are calculated as follows

$$\begin{aligned} K_H &= M_H (2 \pi \times f_H)^2 \\ &= 15393.32E3 (2 \pi \times 0.333)^2 \\ &= 6.7388 \times 10^7 \text{ N/m} \end{aligned}$$

$$\begin{aligned} C_H &= 2 M_H \zeta (2 \pi \times f_H) \\ &= 2 (15393.32E3)(0.05)(2 \pi \times 0.333) \\ &= 3.22074 \times 10^6 \text{ N.s/m} \end{aligned}$$

The vertical frequency of isolated system is assumed to be 21 Hz. Therefore, the vertical stiffness and damping value are calculated as follows

$$\begin{aligned}
 K_V &= M_V (2 \pi \times f_V)^2 \\
 &= 14883E3 (2 \pi \times 21.0)^2 \\
 &= 25.91 \times 10^{10} \text{ N/m}
 \end{aligned}$$

$$\begin{aligned}
 C_V &= 2 M_V \zeta (2 \pi \times f_V) \\
 &= 2 (14883E3)(0.03)(2 \pi \times 21.0) \\
 &= 11.78258 \times 10^7 \text{ N.s/m}
 \end{aligned}$$

### 3.2 Vertical seismic analysis model

The vertical seismic analysis model is the same as the horizontal seismic analysis model except for the fluid added mass effects invoked by the fluid gaps. The total weight of the ABTR reactor structure used in the seismic analysis model is 14,883 tons, which is approximately similar with an estimated 11,000 tons.

## 4. Coupled modal characteristics of ABTR

The simple stick model verified through the detailed 3-dimensional finite element models and the joint stiffness models are assembled to make an overall coupled seismic analysis model as shown in Fig. 2. The term of ‘‘Coupled’’ is defined as a descriptive term for mathematical models of structures and items of plant equipment that are interconnected and which, because of their coupling, influence the dynamic response of each other.

As described in the above sections, there are three coupled seismic analysis models in the direction of horizontal  $X$ ,  $Y$ , and vertical  $Z$  due to the non-axisymmetric geometry of reactor internals and the arrangement of main components inside reactor vessel. In this report, the modal analyses are performed for each direction of a coupled seismic analysis model to verify the coupled modal characteristics with and without seismic isolation system.

For the horizontal  $X$ -direction, the fundamental natural frequency is 4.6 Hz, presenting the coupled mode shape between IHX and reactor internals as shown in Fig. 18(a). The coupled mode between the reactor vessel, core, reactor internals, and primary components is shown in Fig. 18(b) with frequency of 6.8 Hz. As shown in the figure, the reactor vessel has an in-phased coupled mode shape. The fundamental natural frequency of a reactor building is 8.8 Hz, slightly coupled with containment vessel and reactor components as shown in Fig. 18(c).

For the horizontal  $Y$ -direction, the fundamental natural frequency is 1.8 Hz, presenting the IHX vibration mode shape horizontally coupled with a reactor internal structure as shown in Fig. 19(a). This coupled natural frequency increases much higher compared with 0.76 Hz for a single IHX component no coupling with reactor internal structure. The second mode is a coupled IHX and reactor internals with 4 Hz as shown in Fig. 19(b). The coupled reactor vessel has 8 Hz natural frequency as shown in Fig. 19(c).

When introducing the seismic isolation system of 0.333 Hz, the whole reactor building and components are in a rigid body motion as shown in Fig. 20. This means that the horizontal stiffness of seismic isolator is flexible enough to make the fundamental natural frequencies for all reactor system and components sufficiently higher than the seismic isolation period of three seconds.

When there is no sodium fluid effect, i.e. in air condition, the fundamental frequency of the IHX

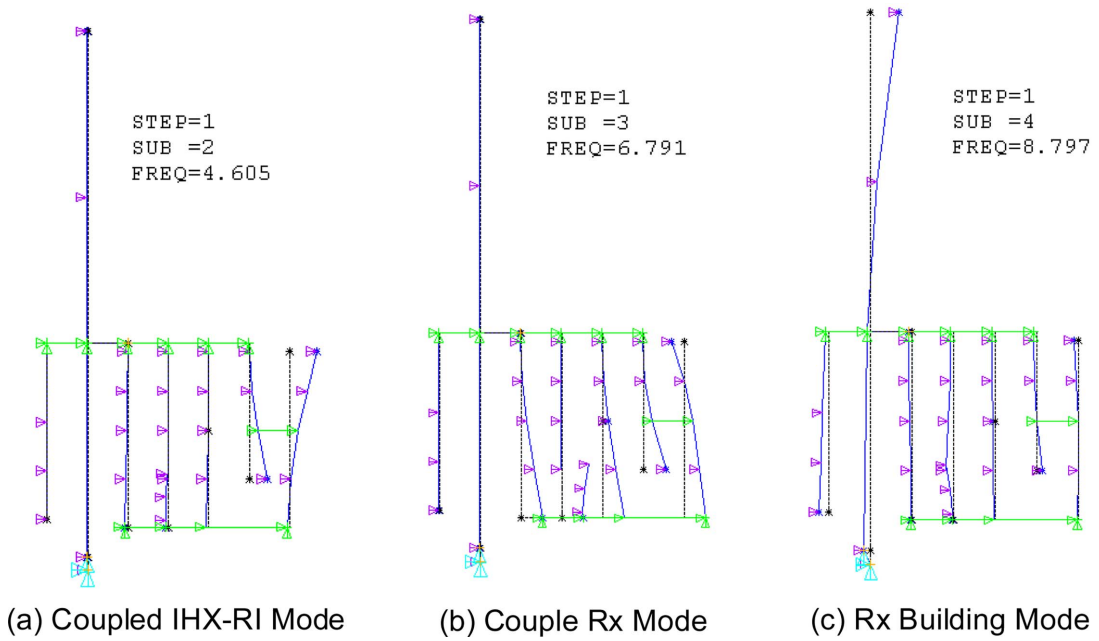


Fig. 18 Coupled mode shapes in X-direction

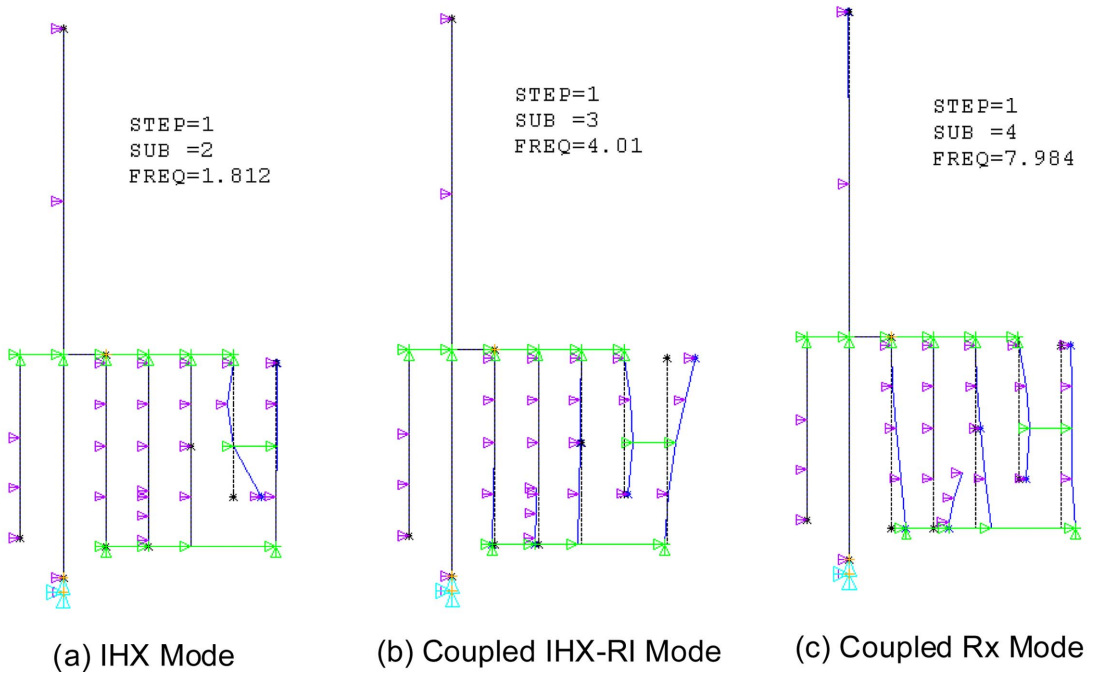


Fig. 19 Coupled mode shapes in Y-direction

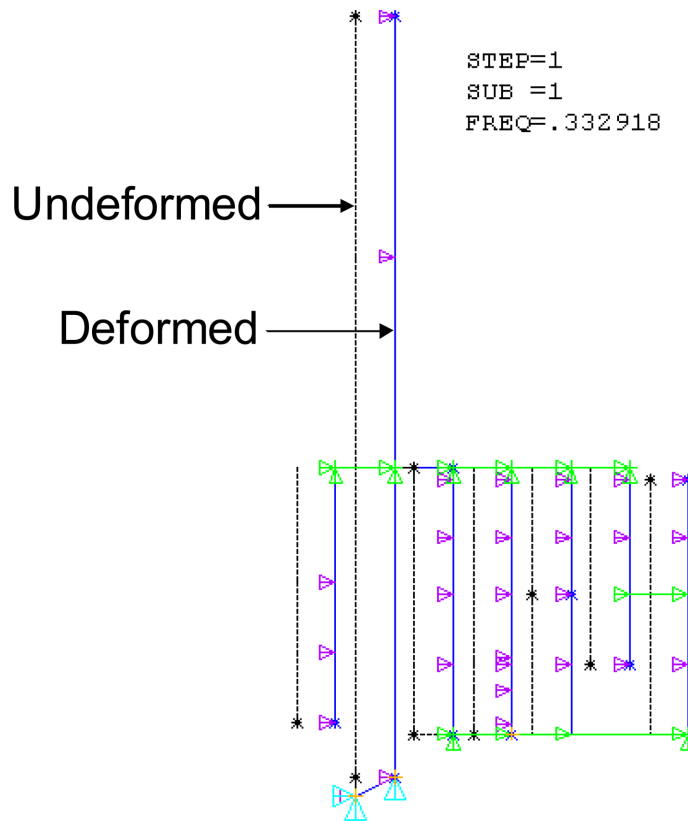


Fig. 20 Seismic isolation mode shape (rigid body motion)

component itself is 1.44 Hz larger than seismic isolation frequency of 0.33 Hz. However, in sodium-condition, the frequency falls down to 0.32 Hz close to seismic isolation design frequency. It is likely that the seismic response of IHX can be greatly amplified due to severe coupling effects between isolation devices and the IHX due to sodium fluid effects. However, as described in section 4 and Fig. 1, four IHX components are horizontally coupled together with reactor internal structures, then the coupled frequency of IHX components increase up to 4.61 Hz for  $X$ -direction and 1.81 Hz for  $Y$ -direction. Therefore, the coupled effects between the isolation devices and the sodium fluid are little in this seismic model.

For the vertical seismic analysis model, the core assembly has the lowest fundamental natural frequency of 2.2 Hz as shown in Fig. 21(a). This natural frequency is located in range of strong seismic input spectrum frequencies. Therefore, large seismic response amplification is expected for vertical core seismic motions. Fig. 21(b) presents the second mode shape of 18.7 Hz, which is caused by assumed vertical seismic isolation frequency of 21 Hz. This mode reveals a coupled reactor building and reactor structures in-phase direction. The third mode shape is shown in Fig. 21(c), which is an out-of-phase motion between the reactor building and the reactor.

Table 3 presents the summary of horizontal modal analysis results for the detailed 3-dimensional finite element models, the simple stick models, and the assembled seismic stick model.

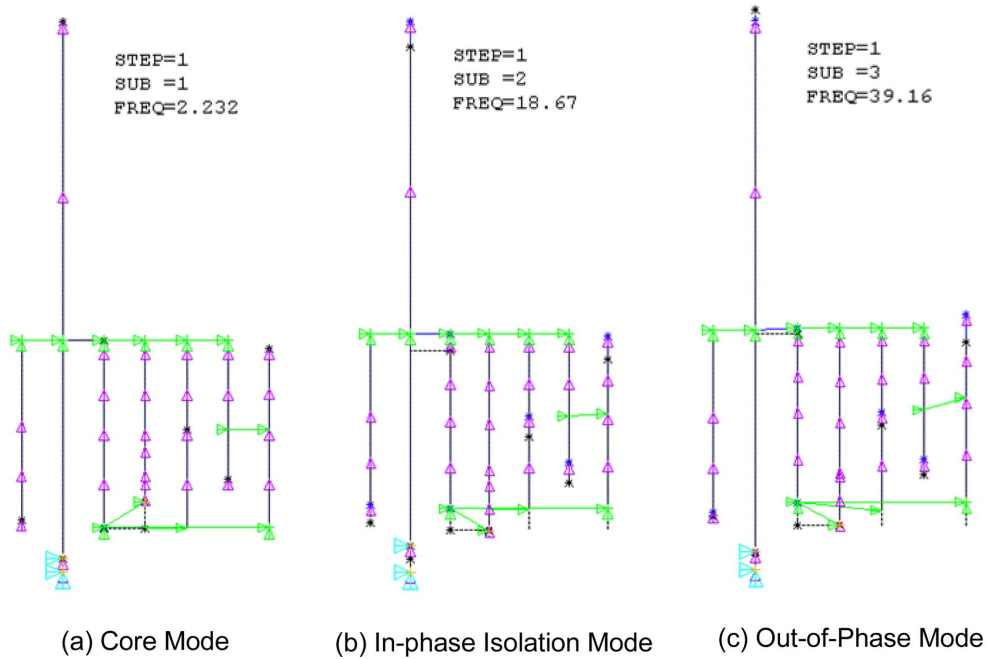


Fig. 21 Vertical mode shape of ABTR

Table 3 Summary of couple modal analyses of ABTR

Parts	Detailed FE Model (Hz)		Simple Stick Model (Hz)		Coupled Stick Model (Hz)	
	X	Y	X	Y	X	Y
Reactor Vessel	13.68	13.68	13.65	13.65	6.79	7.97
Reactor Internals	4.95	4.25	4.98	4.26	4.61	4.01
IHX	0.32	0.76	0.32	0.76	4.61	1.81
Pump	4.98	4.98	4.94	4.94	6.79	7.97
UIS	13.11	13.11	13.16	13.16	13.16	13.16
Core	10.41	10.41	10.77	10.77	6.79 (10.77)	7.98 (10.77)
CV	26.72	26.72	26.88	26.88	26.83	26.83
Reactor Building	8.34	8.34	8.36	8.36	8.80	8.70

## 5. Seismic time history response analyses

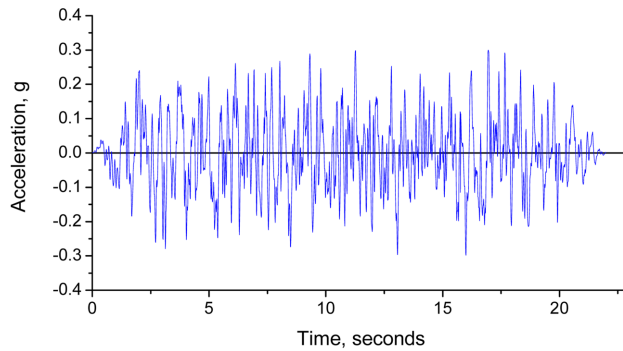
The main purposes of the seismic time history response analyses are to generate design floor response spectrum for seismic design of reactor components and structures and to investigate the seismic deflection limits for functional requirements. To investigate the performance of the seismic isolation design, the analyses both for seismic isolation and non-seismic isolation design are performed in this paper.

### 5.1 Seismic design loads

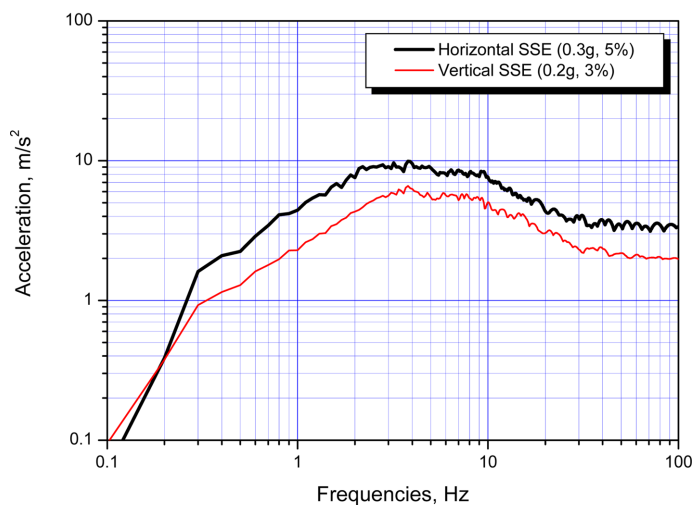
The horizontal seismic design loads used in seismic time history analyses are the artificially generated OBE (Operation base Earthquake, 0.15 g) and SSE (Safe Shutdown Earthquake, 0.3 g) time histories to calculate seismic response of safety-related nuclear structures. The vertical SSE load is 0.2 g. These input motions contain a sufficient number of peaks as shown in synthetic acceleration time histories of Fig. 22(a) and envelop the NRC Reg.1.60 seismic design spectrum criteria (NRC 1973). Fig. 22(b) presents acceleration response spectra for SSE input ground motions in directions of horizontal and vertical motions. The frequency contents of peak spectrum are ranged from 2 Hz to 10 Hz for horizontal direction and from 3 Hz to 10 Hz for vertical direction.

The general assumptions used in seismic time history response analyses are as follows;

- 3% and 5% critical damping ratio for horizontal OBE and SSE, respectively
- 3% critical damping ratio both for vertical OBE and SSE
- 5 % critical damping ratio for seismic isolators



(a) Synthetic acceleration input motion



(b) Seismic design spectra

Fig. 22 Seismic input time histories for SSE

- No rotational degree of freedom of upper and lower basemat
- No coupling effects between horizontal, vertical and torsional motions
- Neglect rocking motion due to seismic isolation system

The total time of input motion used in analyses is 21 seconds and the integration time interval is 0.01 seconds.

## 5.2 Results and discussions

### 5.2.1 Relative displacement responses

Table 4 presents the summary results of the maximum seismic deflection responses both for seismic isolation and non-seismic isolation design. As shown in the table, the maximum horizontal relative deflections between the reactor building and the basemat are 217 mm for OBE and 400 mm for SSE in case of a seismic isolation design. The calculated maximum deflection value for SSE load exceeds the specified ABTR seismic deflection limits of 300 mm. This is mainly caused by the too low seismic isolation period of 3 seconds (0.333 Hz). When the seismic isolation design frequency slightly tends to increase up to 0.5 Hz, the maximum relative deflection response of reactor building can be reduced down to 254 mm and meet the design requirement.

Restricting the horizontal relative seismic deflection response between the UIS and the core assemblies is one of important functional design requirements to protect the driveline against excessive bending deflection which can increase the contact loads and scram time. If relative deflections exceed the clearances available in the normal operating configuration when the drivelines are constrained by both the UIS and the core, the interference loads can permanently deform the drivelines and the enveloping components with adverse effect of the control rod operation. Such interference has to be precluded by limiting the relative seismic deflection. This can govern the UIS seismic design. The calculated maximum relative deflections for the seismic isolation design are small as 0.7 mm for OBE and 1.2 mm for SSE. In case of the non-seismic isolation design, the seismic deflections significantly increase as 4.7 mm for OBE and 7.9 mm for

Table 4 Summary of maximum relative displacement responses

(unit: mm)

Design Condition	Load	Rx Building	UIS/Core		RI/RV		RV/CV		Core/CSS		Closure/UIS		Closure/Core
		HX	HX	HY	HX	HY	HX	HY	HX	HY	HX	HY	VZ
Seismic Isolation	OBE	217	0.7	0.7	0.6	0.8	1.2	1.1	0.3	0.3	0.8	0.7	13.7
	SSE	<b>400</b> (254*)	1.2	1.2	1.1	1.4	2.2	2.0	0.6	0.6	1.5	1.3	27.3
Non-Isolation	OBE	-	<b>4.7</b>	4.5	4.1	4.8	6.3	5.1	2.3	2.5	3.8	3.2	13.5
	SSE	-	<b>7.9</b>	7.3	6.0	8.9	10.3	9.3	4.0	3.9	6.1	5.7	26.9

\* : In case of 0.5Hz isolation system

Note: (a) UIS deflection limit (PRISM) :

- Non-seismic isolation = 4.6 mm
- 0.5Hz isolation system = 11.3 mm
- 1.0Hz isolation system = 14.2 mm

(b) Maximum relative displacement (ABTR) = 300 mm

SSE. These responses exceed the UIS deflection limit of 4.6 mm for SSE required in PRSIM design.

The maximum relative deflection between the reactor vessel and internal structure is 1.4 mm for SSE load in the seismic isolation design. Considering 73 mm design gap between them, the design margin is sufficient for seismic deflections. The maximum core deflection is less than 1 mm for a seismic isolation design and 4 mm for a non-seismic isolation design, respectively.

The relative vertical displacement between the core and the reactor head is an important factor to estimate the variation of a reactivity insertion during seismic events. For OBE condition, the maximum vertical relative displacements are 13.7 mm for the seismic isolation design and 13.5 mm for the non-seismic isolation design, respectively. For SSE condition, the maximum vertical relative displacements between the core and the reactor head are 27.3 mm for a seismic isolation and 26.9 mm for non-seismic isolation design, respectively. Due to the vertical natural frequency of the seismic isolator, the maximum seismic response for seismic isolation design slightly increases compared with that for non-seismic isolation design case.

### 5.2.2 Seismic floor response spectra (FRS)

The response spectrum is defined as the maximum response of single degree of freedom systems of varying frequency (or period) to a given input support excitation. The equation describing the response of the system in terms of the relative displacement ( $X$ ) is

$$\ddot{X} + 2\xi_n\omega_n\dot{X} + \omega_n^2X = -\dot{X}_o$$

where

$X$  = Relative displacement

$\omega_n$  = Natural frequency of the system

$\xi_n$  = Ratio of viscous damping to critical damping

$X_o$  = Input base excitation displacement

The solution of above equation for the maximum response,  $X_{\max}$ , at various frequencies results in the spectral response curve. To generate a response spectrum from displacement time-history and frequency data, the damping values are used to be five percent for SSE and three percent for OBE in horizontal directions and three percent for vertical direction regardless of seismic load conditions. The frequency interval for generation of design response spectra is 0.1 Hz throughout the frequency range of 0.1 Hz to 100 Hz, which is sufficiently small to produce accurate response spectra including significant peaks normally expected at the natural frequencies of the supporting structures.

Fig. 23 presents the comparison of the calculated FRS for various locations in horizontal directions. In case of a seismic isolation design, response spectrum curves are almost same for  $X$  and  $Y$ -directions, and there are no response amplifications at all reactor building and reactor system due to almost rigid body motion. The peak responses occur only at the 0.33 Hz corresponding to the horizontal seismic isolation. However, in case of a non-seismic isolation design, seismic responses are significantly amplified and the maximum peak acceleration responses occur at core assembly as expected in dynamic characteristics. The top of a reactor building reveals a peak response at 8.4 Hz corresponding to the fundamental natural frequency regardless of directions. In horizontal  $X$ -direction of OBE load, the amplification factors for zero period acceleration are 5.7 for top of core assembly, 3.3 for a reactor vessel bottom, 2.8 for UIS bottom, and 2.6 for a top of

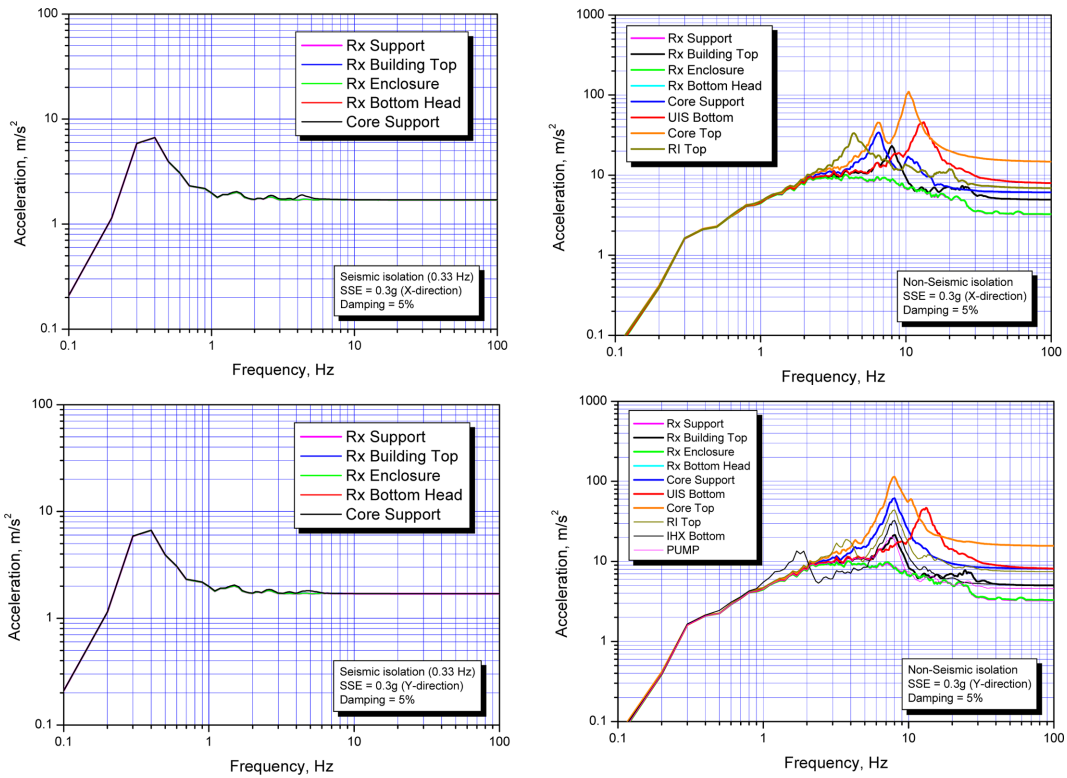


Fig. 23 Comparison of floor response spectra in horizontal directions

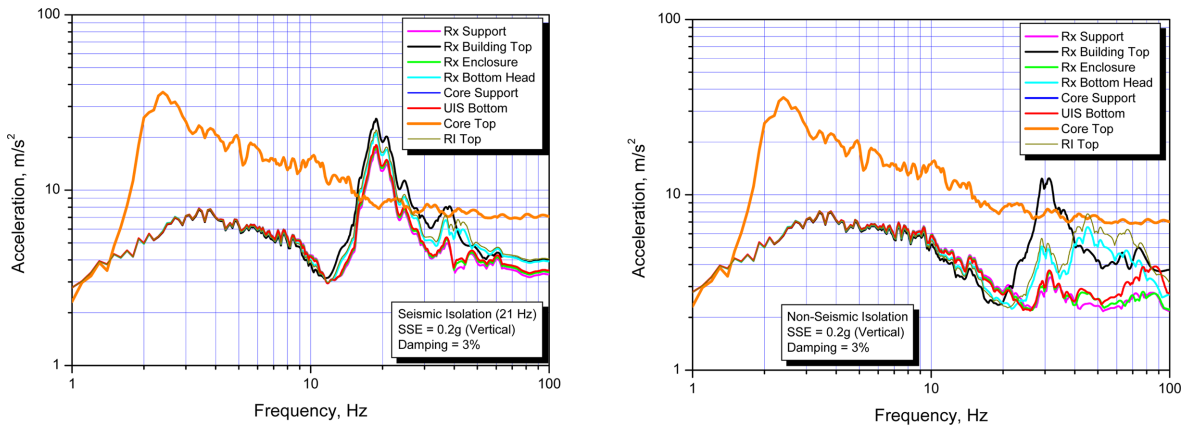


Fig. 24 Comparison of floor response spectra in vertical direction

reactor internals. For a horizontal *Y*-direction, the IHX reveals a peak response at 1.8 Hz corresponding to the fundamental natural frequency of IHX itself. Fig. 24 reveals the comparison of the calculated FRS for various locations in vertical directions. As shown in results, the maximum peak response occurs at core support structure due to its flexible vertical stiffness as discussed in Section 4. For vertical responses of other locations, we can see that the seismic isolation design has

a disadvantage due to additional vertical modal frequency of seismic isolator. This can invoke seismic design issues in a vertical direction for a subsystem.

The design response spectra, which can be used to be an input motion for subsystem seismic analysis, are defined from the calculated floor response spectra. According to the ASCE standard (ASCE 1986), the floor response spectra shall be broadened to account for uncertainties in response due to the uncertainties in supporting structure frequencies and soil-structure interaction analysis. The minimum broadening shall be  $\pm 15\%$  at each frequency in the amplified response region.

## 6. Conclusions

In this paper, the technologies to develop the seismic time history analysis model for a pool-type sodium-cooled fast reactor are proposed with detailed descriptions of simple stick models. In developing the seismic stick model, the fluid added mass effects on reactor vessel, internals, and components are considered through detailed finite element analyses for a fluid gap model. From the comparison of the frequency modal analyses with a 3-D finite element model, it is verified that the proposed seismic stick model is in a good agreement with that of the 3-D model. From the deflection limit evaluations by the seismic time history analyses, the performance of the seismic isolation design is proved in terms of acceleration responses but the relative deflection between reactor building and basemat greatly exceeds the functional requirement given in conceptual design due to lower isolation frequency of 0.33 Hz. Therefore, it is recommended to increase the seismic isolation frequency at least up to 0.5 Hz.

## Acknowledgments

This project has been carried out under the Nuclear R & D Program by Ministry of Science and Technology of South Korea.

## References

- ASCE (1986), *Seismic Analysis of Safety-Related Nuclear Structures and Commentary on Standard for Seismic Analysis of Safety Related Nuclear Structures*, American Society of Civil Engineers.
- Chang, Y.I., Finck, P.J., Grandy, C. *et al.* (2006), *Advanced Burner Test Reactor Preconceptual Design Report*, ANL-ABR-1, Argonne National laboratory.
- Forni, M. and Martelli, A. (1994), *Proposal for Design Guidelines for Seismically Isolated Nuclear Plants; Final Report*, Contract ETNU-0031-IT (CCSH).
- Kim, S.O., Lee, J.H. *et al.* (2009), *Development of Basic Key Technologies for Gen IV SFR*, KAERI/RR-3107/2009, Korea Atomic Energy Research Institute.
- Koo, G.H., Sienicki, J.J., Tzanos, C.P. and Moisseytsev, A. (2009), "Creep-fatigue design evaluations including daily load following operations for the advanced burner test reactor", *Nucl. Eng. Des.*, **239**, 1750-1759.
- Koo, G.H. and Lee, J.H. (2003), "Development of FAMD code to calculate the fluid added mass and damping of arbitrary structures submerged in confined viscous fluid", *KSME Int. J.*, **17**(3), 457-466.
- Lo Frano, R. and Forasassi, G. (2009), "Conceptual evaluation of fluid-structure interaction effect coupled to a seismic event in an innovative liquid metal nuclear reactor", *Nucl. Eng. Des.*, **239**, 2333-2342.
- Lo Frano, R., Pugliese, G. and Forasassi, G. (2010), "Preliminary seismic analysis of an innovative near term

- reactor: methodology and application”, *Nucl. Eng. Des.*, **240**, 1671-1678.
- Micheli, I., Cardini, S., Colaiuda, A. and Turoni, P. (2004), “Investigation upon the dynamic structural response of a nuclear plant on aseismic isolating devices”, *Nucl. Eng. Des.*, **228**, 319-343.
- NRC (1973), *NRC Reg. Guide 1.60, Design Response Spectra for Seismic Design of Nuclear Power Plants*, Revision 1, December.
- Sigrist, J.F., Broc, D. and Laine, C. (2006), “Dynamic analysis of a nuclear reactor with fluid structure interaction Part I : Seismic loading, fluid added mass and added stiffness effects”, *Nucl. Eng. Des.*, **236**, 2431-2443.
- Su, T.C. (1983), “The effect of viscosity on the forced vibrations of fluid-filled elastic shell”, *J. Appl. Mech.*, **50**, 517-524.
- Yang, C.I. and Moran, T.J. (1980), “Calculations of added mass and damping coefficients for hexagonal cylinders in a confined viscous fluid”, *J. Press. Vessel Technol.*, **102**, 152-157.